

# Optical Tweezers: Measuring Piconewton Forces

Mark C. Williams

Northeastern University

Department of Physics and Center for Interdisciplinary Research on Complex Systems

Email: mark@neu.edu

## 1. Introduction

Optical tweezers instruments use the forces of laser radiation pressure to trap small particles. Using various techniques, these trapped particles can then be manipulated and forces on the objects in the trap can be measured. The forces that such an instrument is capable of measuring are of the order of one to 100 piconewtons (pN). While this technique has been used for over 20 years to manipulate and study the properties of micron-sized dielectric particles, it is only recently that this precise force measurement instrument has been applied to the study of biological systems.

This chapter will outline the physics responsible for the trapping and force-measuring capabilities of optical tweezers instruments. The designs of two major types of optical tweezers will be described and the limitations and advantages of each type will be discussed. Detailed designs of instruments and instructions for building optical tweezers will not be given. However, this information can be found in the references at the end of the chapter. After discussing the general properties of optical tweezers, we will describe a few of the many types of experiments that have used these instruments to study the properties of biological systems.

The ability to manipulate single molecules with nanometer precision and to measure forces on these molecules with piconewton accuracy using optical tweezers has opened up several important new areas of study in biophysics. These new single molecule manipulation experiments have allowed us to test physical models describing the properties of DNA in a way that was never before possible. We can now observe the activity of a single enzyme acting on a DNA molecule and watch tiny molecular motors exert forces on biological molecules. We can directly test the effects of DNA binding proteins on the properties of DNA and use these measurements to determine their energy of interaction. A detailed knowledge of individual interactions between molecules is essential for understanding the complex mechanisms involved in real biological processes. Single molecule measurements of these interactions have generated significant new insights into these processes. A few examples of how optical tweezers have been used to study these interactions will be discussed in Section 5 of this chapter.

## 2. Optical trapping of dielectric particles

Radiation pressure is a force per unit area on an object due to the change in momentum of light. All light consists of photons that each have momentum  $\vec{p}$ . For light of specific wavelength  $\lambda$ , the magnitude of the momentum of a single photon is given by

$$|\vec{p}| = \frac{h}{\lambda} \quad (1)$$

The intensity of the light is determined by the number of photons passing through a given area per unit time. The momentum flux of photons from light of intensity given by the pointing vector  $\vec{S}$  is

$$d(d\vec{P}/dt) = (n/c)\vec{S}dA, \quad (2)$$

where  $n$  is the index of refraction,  $c$  is the speed of light,  $\vec{P}$  is the total momentum of the photons, and  $dA$  is an element of area normal to  $\vec{S}$ . Thus, in principle one can directly calculate the force on a given area due to the light momentum flux on that area.

Since the force on a dielectric object is given by the change in momentum of light induced due to refraction of the light by the object, the total force on the object is the difference between the momentum flux entering the object and that leaving the object. The total force on an object due to refraction of light is therefore

$$\vec{F} = (n/c)\iint(\vec{S}_{in} - \vec{S}_{out})dA \quad (3)$$

Thus, if the light coming into a dielectric from a medium of index  $n$  is deflected, changing the direction of  $\vec{S}$  when it exits the dielectric, there is a finite force exerted on the object.

This suggests that light exerts a force on all objects that refract or reflect light. In fact, this is always the case. However, in most situations this force is so much smaller than other forces acting on macroscopic objects that there is no noticeable effect. For example, we can calculate the force due to the change in momentum of light reflecting off of a mirror. In this case,  $\vec{S}_{out} = -\vec{S}_{in}$ , so  $\vec{F} = 2(n/c)\iint(\vec{S}_{in})dA$ . The integral represents the total power of the light, which is usually expressed in Watts. In the simple case of 100% reflection, the force is thus  $F = 2(n/c)W$ , where  $W$  is the intensity of the light in Watts. If all of the intensity of a 60 W light bulb were focused onto a mirror, the force due to radiation pressure would be  $4 \times 10^{-7}$  N. If a 1 kg mirror exerts a force on a scale of 9.8 N, the additional weight due to radiation pressure is clearly negligible. Objects for which this radiation pressure would be significant would have to weigh less than 1  $\mu$ g.

In optical tweezers experiments, the radiation pressure is provided by laser light, while the objects to be manipulated are generally very small. Micron-sized polystyrene spheres of uniform diameter are easily obtained and can be trapped using the forces described by Eq. 3. The example of a mirror outlined above shows how radiation forces can be used to manipulate a small object by applying a small force. In that case, the object is *pushed* by the *reflection* of light from its surface. Radiation forces due to *refraction* can also be used to *pull* a transparent object. A qualitative outline of how this is possible is shown in Figure 1 (adapted from (Ashkin 1998)). Here we trace only two rays of light, denoted rays 1 and 2, which are focused by a lens (or series of lenses that make up a microscope objective). Each ray is refracted at the surface of the bead so that its direction of propagation changes according to Snell's law, which states that  $n_1 \sin(\theta_1) = n_2 \sin(\theta_2)$ , where  $n_1$  is the index of refraction of the medium surrounding the sphere (usually water) and  $n_2$  is the index of refraction of the sphere. Here  $\theta_1$  is the angle of incidence of the ray with respect to a line perpendicular to the surface of the sphere and  $\theta_2$  is the angle with respect to the same line at which the ray propagates within the sphere. Snell's law indicates that the change in direction of the light at the interface of the bead with its surroundings depends strongly on the index of refraction of each medium. Since these experiments are usually done in water,  $n_1$  is 1.33, while  $n_2$  is 1.55 if the sphere is

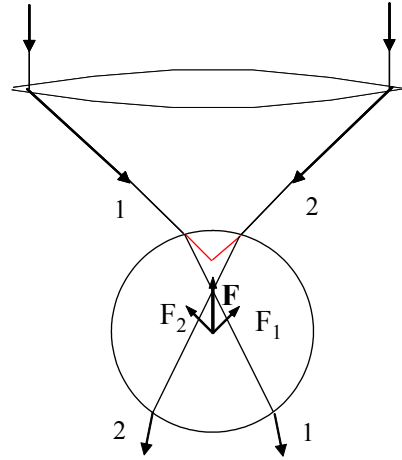


**Figure 1. Schematic diagram showing the force on a dielectric sphere due to refraction of two rays of light, 1 and 2. The resultant force on the bead due to refraction is towards the focus.**

made of polystyrene. The index  $n$  in Eq. 3 represents the medium surrounding the sphere in this problem. The change in direction of the light due to refraction is all contained within the integral in Eq. 3. In general, this equation is difficult to solve. However, for simple cases that can be solved, the qualitative picture shown in Figure 1 holds. Thus, a ray of light impinging on the interface of the sphere in Figure 1 has its direction of propagation, and therefore its momentum, changed by the interaction of the light with the sphere. Since the sphere changes the momentum of the light, an equal and opposite change in momentum of the bead occurs. The resultant force of the light on the sphere due to refraction is always in the direction of the focus of the light (shown as the intersection of two red lines). Thus, in the absence of other forces, the sphere is attracted to the focal point of the light.

The above discussion appears to indicate that simply shining light on a small spot is sufficient to create an optical trap. This is true, but the attractive force due to refraction of the light at the surface of the bead must be sufficient to overcome any other forces acting to push the bead out of the trap. One such force is the force due to reflection at the bead surface, illustrated in Figure 2. Depending on how much light is reflected at the bead surface, the force due to reflection can easily push the sphere out of a weak trap. To overcome this loss mechanism, the optical trap must be designed to have a high trapping force. It is clear from Figures 1 and 2 that the light coming from the edges of the objective lens contributes the most to the trapping force. This is generally true in optical tweezers. In practice, this means that a microscope objective with a high numerical aperture (NA) must be used to generate the greatest trapping force. From the diagram in Figure 3, it is clear that the maximum numerical aperture is  $n$ , where  $n$  is the index of refraction of the medium immediately following the objective. For air, this is one. Therefore, oil immersion objectives, which are designed to have oil between the microscope objective and sample, are often used in optical tweezers instruments. These can have numerical apertures of up to 1.4. The use of high power lasers also maximizes the trapping force.

An alternative optical tweezers design that can easily overcome the loss due to reflection at the bead surface uses a dual-beam design, shown in Figure 4. In this design, two microscope objectives face each other and focus two separate laser beams to the same spot. Since the force due to reflection is approximately the same for each laser, these forces cancel and the trap is stabilized. Dual beam optical tweezers instruments are therefore able to generate higher trapping forces for a given laser power and can be constructed with lower NA microscope objectives. The disadvantage of such an instrument is mainly complexity. Single beam optical tweezers can be constructed using a single laser and a commercial microscope. A dual beam instrument must in general be constructed only from parts of a microscope such as objectives and tube lenses and cannot be easily incorporated into a standard microscope body. In addition, the two laser beams must be aligned to within less than a bead diameter and the resulting measurements must be corrected for errors due to drifts in the relative alignment of the laser beams. Because of these alignment issues, single beam instruments are preferable for trapping beads of diameters less than one  $\mu\text{m}$ .

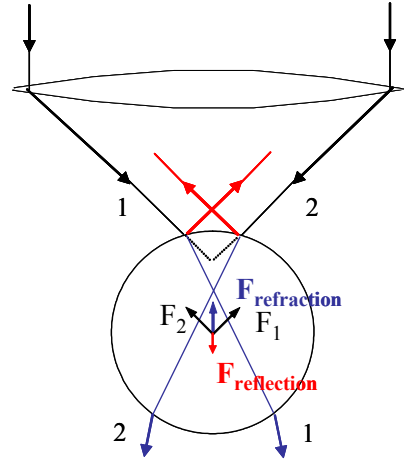


**Figure 2. Schematic diagram showing the force on a dielectric sphere due to both reflection and refraction of two rays of light.**

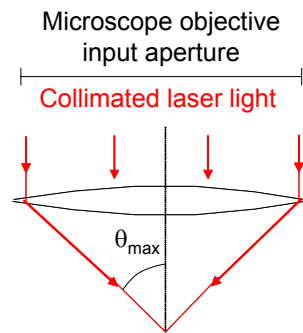


**Figure 3. Collimated light focused by a microscope objective (indicated schematically as a lens). If laser light completely fills the objective input aperture, the maximum angle of light that can be focused is  $\theta_{\text{max}}$ . The numerical aperture (NA) of the objective is  $n\sin(\theta_{\text{max}})$ , where  $n$  is the index of refraction of the medium below the objective.**

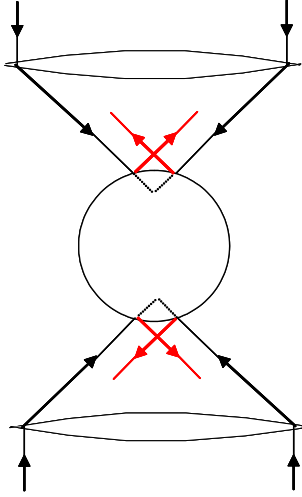


**Figure 4. Schematic diagram of a dual-beam optical trap. The red lines represent light reflected at the surface.**

According to Eq. 3, the maximum optical trapping force due to refraction will occur when  $\vec{S}_{out} \perp \vec{S}_{in}$ . In this case the force in one direction is  $F_x = (n/c) \iint (|S_{in}|) dA = (n/c)W$ . This would represent an optical trap that is of maximum efficiency. In practice, this efficiency is never achieved. Thus, an optical trap is usually characterized as having a quality factor  $Q$ , such that  $\vec{F} = (n/c) \iint (\vec{S}_{in} - \vec{S}_{out}) dA \equiv \vec{Q}(n/c)W$ , where the magnitude of  $\vec{Q}$  varies depending on the direction in which  $\vec{F}$  is measured. Quality factors for optical tweezers can be up to  $Q = 0.3$  perpendicular to the direction of propagation of laser beam (Smith et al. 2002). The quality factor depends strongly on the type of optical trap, the NA of the microscope objective(s), and the size of the trapped bead. If the laser power at the sample is 150 mW, the maximum trapping force is 198 pN for  $Q = 0.3$ . However, depending on the geometry, the actual force in a single beam instrument can be lower in certain directions due to the additional scattering force (Ashkin 1998).

### 3. Measuring small forces with optical tweezers

So far we have seen that forces due to refraction of light can be used to form an optical trap that attracts small polystyrene spheres. While this is interesting, it is only useful if we can make quantitative measurements that take advantage of these new micromanipulation techniques. Fortunately, optical tweezers can be used to directly measure forces on trapped objects. In the previous section, we mentioned that a polystyrene bead that is held at some position away from the focus of the laser beams experiences an attractive force towards the focus. It turns out that this restoring force is in most cases proportional to the distance between the center of the sphere and the focus of the lasers. In other words, optical tweezers force can generally be described by the equation:

$$\vec{F} = -k\vec{x}. \quad (4)$$

Thus, if we can determine the constant  $k$ , referred to as the *trap stiffness*, measuring the position of the bead in the trap determines the force on the bead in the trap. Modern image analysis techniques are able to measure the position of a micron-sized sphere with an accuracy of 10 nm. The trap stiffness varies considerably depending on the design of the optical tweezers and the size of the sphere, but a value of 50 pN/ $\mu\text{m}$  is reasonable. This gives a resolution of 0.5 pN in force measurement. Here the force resolution is increased by decreasing the trap stiffness.

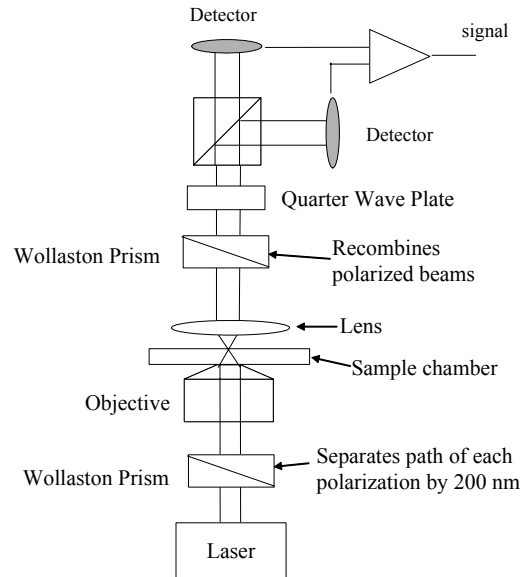


**Figure 5. Schematic diagram of an interferometric detection technique. A single laser beam with two polarization states is separated into two beams of orthogonal polarization. The optical path length of each beam depends on the position of the bead. When the beams are recombined, the intensity of each polarization can be used to determine the position of the bead in the trap.**

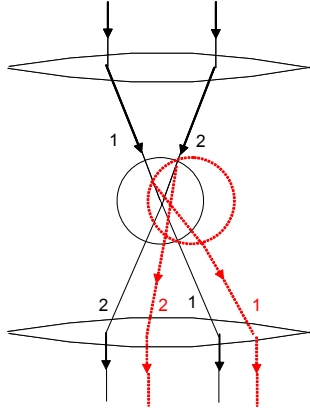


**Figure 6. Measuring the force on a trapped bead.** When a bead is moved from the trap center due to an external force, the trapping laser beam is deflected. If the input aperture of the objective is underfilled in a dual-beam optical tweezers instrument, this deflection can be directly measured using a position-sensitive photodiode detector.

of the light, which can in principle be directly measured by imaging the beam position directly. However, in a single beam optical tweezers instrument, the diameter of the laser light going into the microscope objective is always equal to or greater than the input aperture of the objective. Thus, light that is deflected by the trapped bead is not collected by the objective. However, a dual-beam instrument can sacrifice some trapping force and only fill half of the objective input aperture, as shown in Figure 6. When a force is applied to the bead, the deflection of the laser beam itself can then be directly measured using a position-sensitive photodiode detector (Smith et al. 2002).

To overcome this limitation, other techniques have been used to measure the position of the bead (and therefore the force) more accurately. For example, in a common single beam optical tweezers design, shown in Figure 5, the optical interference pattern between beams displaced by a small distance is used to determine the change in position of a bead in an optical trap. This technique, originally suggested by (Denk and Webb 1990) gives a position measurement resolution of less than one nanometer, so the force resolution is no longer limited by the position measurement. Other techniques use an additional laser for bead position measurement.

In a dual-beam optical tweezers instrument, the trapping laser itself can be used to measure the bead position. As shown in Figure 1, laser light entering and exiting a polystyrene sphere has its momentum changed by the presence of the bead, and this momentum change determines the force exerted on the bead by the light. This change in momentum is equivalent to a change in the direction of propagation

## 4. Force measurement calibration

All of these techniques give us a way to accurately measure a signal that is proportional to the force exerted on a polystyrene bead. In order to determine the force directly, the instrument must be calibrated. In the viscous drag force calibration, we apply a known force and measure the resulting signal as a function of the applied force. If the position of the bead as a function of force is also measured, the results can then be fit to Eq. 4 to determine the trap stiffness  $k$ . In the Brownian motion calibration, we take advantage of our knowledge of the frequency spectrum of position fluctuations in an optical trap to obtain  $k$  directly.

### 4.1 Viscous drag force calibration

The force due to viscous drag on a sphere of known radius can be calculated. If a liquid with viscosity  $\eta$  flows past a sphere of radius  $r$  with velocity  $v$ , the force due to viscous drag  $F_{vis}$  is given by:

$$F_{vis} = \gamma v = 6\pi\eta r v, \quad (5)$$

where  $\gamma$  is the viscous drag coefficient. Since the viscosity of the liquid is known and polystyrene spheres of known radius can be obtained, we can apply a known force if we can measure the velocity of the liquid. This can be done using a video camera by measuring the force signal at a fixed liquid flow velocity and then suddenly turning off the trap and measuring the rate at which the bead moves along with the liquid. A more precise measurement of the flow velocity can be obtained by trapping a bead in an optical trap without flow and then oscillating the cell holding the liquid that surrounds the trapped bead at a fixed frequency and amplitude. If the position of the cell as a function of time is given by

$$x = x_0 \sin(\omega t) \quad (6)$$

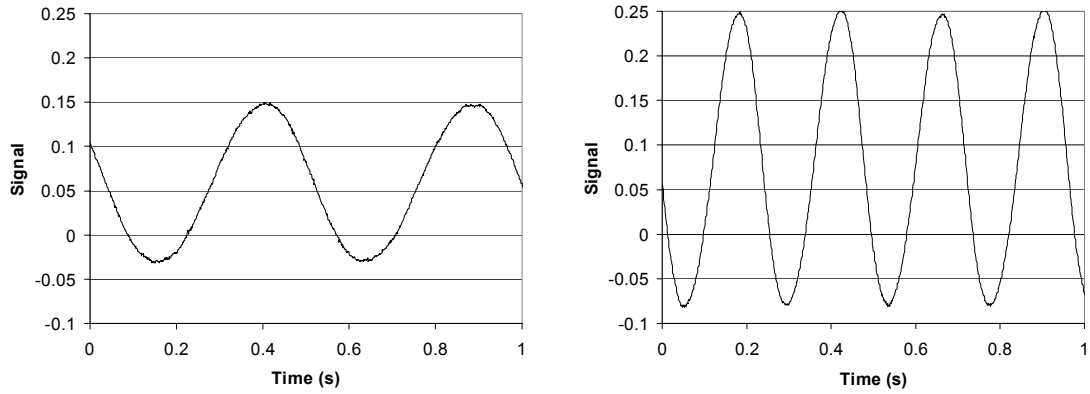


**Figure 7. Output signal from photodiode detectors measuring the trapping laser position as a function of time in a dual-beam optical tweezers instrument. The signal on the left is observed when the liquid surrounding the trapped bead is oscillated at a frequency of 2 Hz according to Eq. 6. The signal on the right is observed when the liquid is oscillated at 4 Hz with the same amplitude. Note that the resulting signal amplitude doubles when the frequency is doubled.**

then the velocity of the cell (and therefore the liquid surrounding the bead) is

$$v = \omega x_0 \cos(\omega t), \quad (7)$$

and the force due to viscous drag on the trapped bead is

$$F_{vis} = 6\pi\eta r \omega x_0 \cos(\omega t). \quad (8)$$

In this case all of the quantities on the right side of Eq. 8 are known, so we know the applied force as a function of time. The measured signal  $S$  as a function of time will be

$$S = A \omega \cos(\omega t). \quad (9)$$

An example of the signal obtained as a function of time with a dual-beam optical tweezers instrument is shown in Figure 7. One can then measure this signal at several frequencies, determine the amplitude  $A\omega$  according to Eq. 9 and fit the resulting data to a straight line to obtain a value for  $A$  with a measured error equal to the standard deviation of the fit. Substituting Eq. 9 into Eq. 8 gives

$$F = \frac{6\pi\eta r x_0}{A} S \equiv D \cdot S \quad (10)$$

We have now obtained the calibration factor  $D$ . Whenever a signal  $S$  is detected with a bead in the trap, we can directly calculate the force on the bead using Eq. 10.

## 4.2 Brownian motion calibration

Another technique that is often used to calibrate optical tweezers instruments is measurement of the Brownian motion of a captured bead. An isolated bead in an optical trap experiences random forces due to thermal fluctuations. The equation of motion of the trapped bead can be expressed as (Gittes and Schmidt 1998)

$$\gamma \frac{dx}{dt} + kx = F(t), \quad (11)$$

where  $\gamma$  is the coefficient of viscous drag (Eq. 5) and  $k$  is the spring constant of the optical trap. If  $F(t)$  is due to thermal fluctuations, it is random and has an average value of zero and its power spectrum is constant, such that

$$|F(f)|^2 = 4\gamma k_B T. \quad (12)$$

The solution to Eq. 11 can be obtained by taking the Fourier transform of both sides, which yields

$$2\pi\gamma(f_c - if)X(f) = F(f), \quad (13)$$

where  $f_c = (k/2\pi\gamma)$ . Taking the modulus of Eq. 13 and using Eq. 12 gives

$$|X(f)|^2 = \frac{k_B T}{\gamma(f_c + f)^2}. \quad (14)$$

This gives the frequency dependence of fluctuations, or the power spectrum, of the position of a bead in an optical trap. An example of an ideal (calculated) power spectrum is shown in Figure 8. The position fluctuations are approximately constant at low frequencies until  $f_c$  is reached, at which point the slope of the power spectrum changes significantly. Thus, measurement of the fluctuations in the position of a bead in an optical trap due to Brownian motion can be used to determine  $f_c$ . Therefore, from Eq. 13 this is a measurement of the trap stiffness,  $k$ , which allows us to determine the force on a bead in the trap directly from its change in position using Eq. 4.

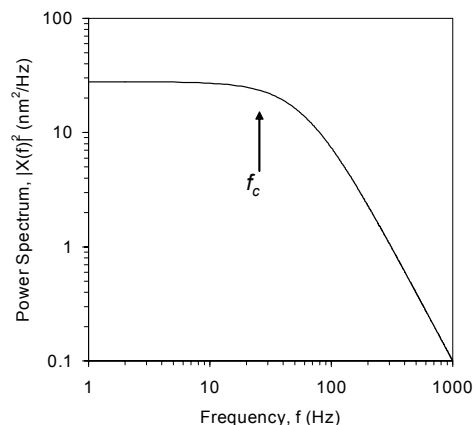


**Figure 8. Ideal power spectrum of a bead in an optical trap. The power spectrum can be used to determine the stiffness of the trap.**

## 5. Measuring forces on single molecules

We have shown that optical tweezers instruments can be used to precisely measure piconewton forces and nanometer position changes of polystyrene spheres. Is this useful? It turns out that this capability can be very useful when combined with a little biochemistry. We can now precisely manipulate micron-sized polystyrene beads, so if we can find a way to attach single molecules to these beads we can study the forces acting on the molecules under various conditions and use these results to model their physical behavior. This gives us two major advantages. First, we can isolate a single molecule and simplify the system that we are studying significantly in the absence of interactions between these molecules that might complicate the analysis. Second, we can measure the properties of a single molecule, thus avoiding the configurational averaging that always takes place in a bulk experiment, as outlined in chapter one of this volume of the Biophysics Textbook Online.

While these single molecule manipulation techniques have been used for a wide variety of experiments, I will focus on one major type of study that has been done using optical tweezers. This is the study of the properties of single DNA molecules and molecules that interact with single DNA molecules. By attaching single DNA molecules to polystyrene spheres and using optical tweezers, researchers have investigated a wide range of important biological interactions in a way that was not previously possible. These studies have revealed important information about the biophysical properties and dynamic structures of both double-stranded and single-stranded DNA (Allemand *et al.* 1998; Baumann *et al.* 2000; Baumann *et al.* 1997; Clausen-Schaumann *et al.* 2000; Cluzel *et al.* 1996; Leger *et al.* 1999; Smith *et al.* 1996). They have revealed the kinetics of DNA polymerase (Maier *et al.* 2000; Wuite *et al.* 2000) and RNA polymerase (Davenport *et al.* 2000; Wang *et al.* 1998; Yin *et al.* 1995) activity. They have demonstrated the ability of topoisomerase enzymes to release a single supercoil in a DNA molecule (Strick *et al.* 2000). These

techniques have been used to determine the thermodynamic properties of DNA (Williams *et al.* 2001c), the energetics of DNA-protein interactions (Williams *et al.* 2001a), and the kinetics of DNA binding proteins (Hegner *et al.* 1999). Researchers have even directly observed the packaging of a single DNA molecule into a virus capsid (Smith *et al.* 2001). Similarly, a recent study has shown that RNA stretching can be used to determine the structure of an RNA molecule and to measure the thermodynamics of RNA folding (Liphardt *et al.* 2001).

## 5.1 Molecular motors acting on single DNA molecules

A significant amount of work has been done using optical tweezers to study the interaction of the the *E. coli* RNA polymerase enzyme with DNA (Davenport *et al.* 2000; Wang *et al.* 1998). RNA polymerases are enzymes that copy a DNA sequence to create single-stranded messenger RNA (mRNA) in a process referred to as *transcription*. The mRNA is then used by the ribosome to create a specific protein in a process called *translation*. Since the polymerase incorporates NTP (where N refers to any of the four RNA ribonucleotides in the mRNA sequence) into the nascent mRNA molecule, energy is released. This energy is used to move the polymerase along the DNA molecule and read the DNA sequence. RNA polymerases are molecular motors because they use energy to create motion and generate forces in the cell. The forces generated by this motor and the forces required to stall the motor have been directly measured using optical tweezers instruments. In addition, specific stall sites were identified at low forces. The average polymerization velocity (i.e. the rate of mRNA creation) was independent of tension up to 25 pN, at which point transcription was reversibly stalled. Figure 9 shows how optical tweezers can be used to perform these studies. In most of these types of experiments, a single polystyrene bead is held in an optical trap with a single DNA molecule attached. The methods of attachment used vary, but a typical type of attachment is to purchase streptavidin-coated beads and use DNA labeled on one end with biotin. In this particular experiment, the RNA polymerase itself is attached to another surface, which is then moved to stretch the DNA that is tethered between that surface and the trapped bead. In (Davenport *et al.* 2000), the RNA polymerase is attached to another polystyrene bead, which is held on the end of a glass micropipette. In order to stretch the DNA molecule, thus exerting a force opposing transcription, the glass micropipette is moved to a specific position or is moved until a specific force on the bead in the optical trap is observed. In the experiments of (Wang *et al.* 1998), the RNA polymerase is attached to a cover slip and the cover slip is moved in order to exert stretching forces. In the initial configuration of a tethered bead/DNA complex, transcription is stalled (i.e. there is no transcription). When the complex is tethered, high concentrations of NTP are added to allow transcription to begin. The results of these studies show that RNA polymerase is a strong molecular motor that is able to exert forces up to 25 pN during transcription, but which often stops transcribing at specific sequences, even when very little force is applied. These results help to explain the role of sequence-dependent pausing in transcriptional regulation.

Experiments have also been reported in which *DNA* polymerase activity was monitored using optical tweezers. (Wuite *et al.* 2000) measured the effect of applied force on the ability of T7 DNA polymerase to convert single-stranded DNA (ssDNA) to double-

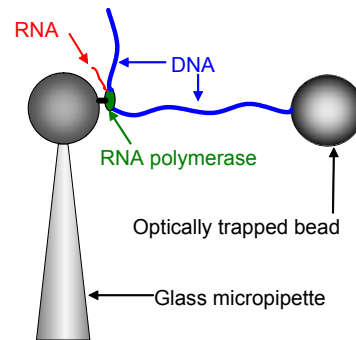


**Figure 9. Schematic diagram of an optical tweezers experiment to measure the transcription forces generated by *E. coli* RNA polymerase. Based on the experiments described in (Davenport *et al.* 2000).**

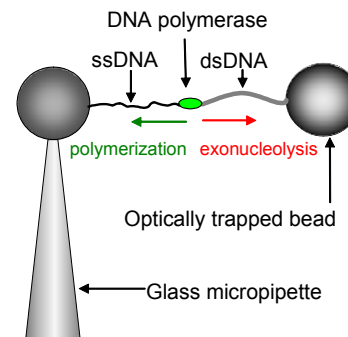


**Figure 10. Schematic diagram of an optical tweezers experiment to measure the polymerization forces generated by T7 DNA polymerase. Based on the experiments described in (Wuite *et al.* 2000).**

stranded DNA (dsDNA), as shown in Figure 10. In contrast to the measurements of RNA polymerase, this study showed that the polymerization velocity of T7 DNA polymerase was very sensitive to tension (i.e. applied stretching force). In addition, production of dsDNA stalled at 34 pN, while higher forces induced fast 3'-5' exonucleolysis (creating ssDNA from dsDNA). In a related study, (Maier et al. 2000) studied replication by the DNA polymerases Sequenase and Klenow, obtaining similar results using magnetic tweezers. Single molecule studies have provided direct measurements of the capabilities of the powerful molecular motors associated with the important biological processes of transcription and replication.

## 5.2 Using single molecule stretching to investigate the biophysical properties of nucleic acids

In order to understand biological processes involving nucleic acids such as DNA replication and repair, as well as RNA transcription and translation, it is important to understand the behavior of nucleic acids under the wide variety of conditions that are present in the cell. Single molecule studies provide a new way of measuring the important properties of nucleic acids that govern these processes. Simple measurements of the forces required to stretch single DNA molecules allow us to study several phases of molecular behavior and to measure thermodynamic quantities associated with conversion of nucleic acids from one structure to another. For example, in the processes of RNA transcription and DNA replication, the base sequence of a dsDNA molecule must be read in order to create a complementary RNA or DNA molecule. In order to read

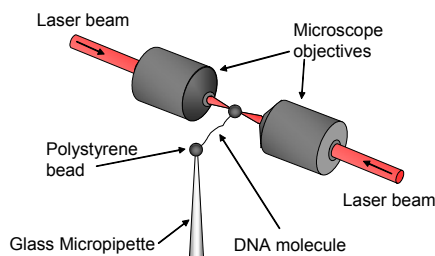


**Figure 11. Schematic diagram of an experiment to stretch single DNA molecules in a dual-beam optical tweezers instrument.**

and copy the base sequence, the bases must be broken. The transition from dsDNA to ssDNA, in which the bases that form the double helix are broken, is referred to as a “helix-coil transition.” Our experiments indicate that a measurement of the DNA helix-coil transition can be obtained at any temperature by measuring the forces required to stretch DNA. In these experiments, a single molecule of  $\lambda$ -DNA is stretched between two polystyrene beads as shown in Figure 11.

As a single molecule of dsDNA is stretched beyond its B-form contour length (about 0.34 nm), the force required to stretch the molecule increases dramatically, as shown in Figure 11. *If one end of the DNA molecule is allowed to rotate freely*, at about 65 pN, a cooperative overstretching transition occurs, in which very little additional force is required to stretch the molecule to 1.7 times its contour length (Cluzel et al. 1996; Smith et al. 1996). To describe this transition, a model of overstretched DNA as a new double-stranded form of DNA, referred to as S-DNA, was proposed (Cluzel et al. 1996). While these models did predict an overstretching transition, the predicted transition was less cooperative and at a higher force than that observed experimentally (Konrad and Bolonick 1996; Lebrun and Lavery 1996; Olson and Zhurkin 2000). Rouzina and Bloomfield (Rouzina and Bloomfield 2001a; Rouzina and Bloomfield 2001b) have proposed an alternative model for DNA overstretching as a force-induced melting process. In this model, the base pairs holding the two DNA strands together break as the DNA unwinds during the transition. This model was shown to be consistent with all available data on the dependence of DNA overstretching on changes in solution conditions such as ionic strength and temperature. It has also been shown that poly(dG-dC)poly(dG-dC) has an overstretching transition about 30 pN higher than poly(dA-dT)poly(dA-dT) (Rief et al. 1999). This result is consistent with the difference in melting temperature between these molecules. However, the authors also observed an additional strand separation transition at forces higher than the overstretching force. In a later work (Clausen-Schaumann et al. 2000), they showed that this

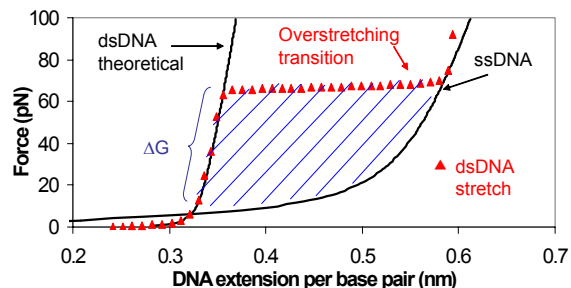


**Figure 12. Force-extension curves for single molecules of dsDNA (red triangles) and ssDNA (right black line). A theoretical curve for dsDNA is shown as the left black line. The overstretching transition appears to be a transition from dsDNA to ssDNA.**

strand separation force depended on the rate at which the dsDNA was stretched, while the overstretching transition did not depend on the pulling rate. In the force-induced melting theory, the overstretching transition is an equilibrium melting transition, while the second transition at higher force is a non-equilibrium strand separation transition, during which the last base pairs holding the two strands together are irreversibly broken. A rate-dependent force is expected when single bonds are irreversibly broken (Evans and Ritchie 1997). If the force-induced melting model is correct, the area between the stretching curves for dsDNA and ssDNA, shown in Figure 12, gives the helix-coil transition free energy. Measuring DNA overstretching is then a powerful new tool for measuring the thermodynamic properties of this transition at any temperature.

To test the force-induced melting model, Williams *et al.* measured DNA overstretching as a function of pH (Williams *et al.* 2001b). Since extremely high and low pH lower the melting temperature of dsDNA, the overstretching force should also decrease if melting occurs during the transition. This decrease in the overstretching force was demonstrated, and the fitted value of the change in entropy of DNA upon melting was in agreement with calorimetric measurements of this parameter at room temperature. As a further test, Williams *et al.* also measured the temperature dependence of DNA overstretching (Williams *et al.* 2001c). While their data were consistent with earlier measurements using AFM (Clausen-Schaumann *et al.* 2000), the high resolution data obtained using optical tweezers allowed them to directly calculate the helix-coil transition free energy as a function of temperature from the force-extension curves. The resulting parameters describing this temperature dependence, which are the heat capacity of DNA upon melting as well as the entropy upon melting at the melting temperature, were in very good agreement with independent calorimetric measurements of these parameters. Finally, measurements of the monovalent salt dependence of DNA overstretching showed that the

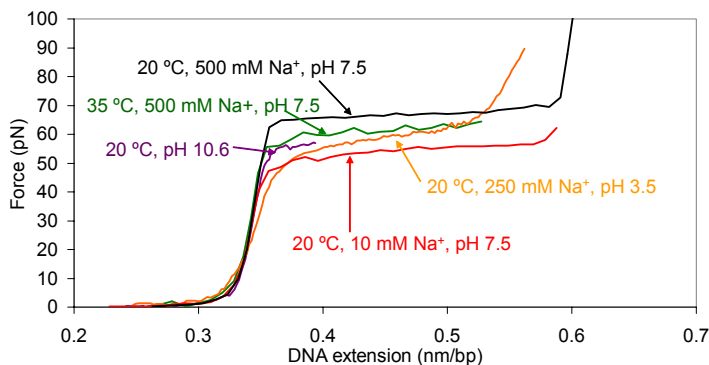


**Figure 13. Force-extension curves for single molecules of dsDNA (red triangles) and ssDNA (right black line). A theoretical curve for dsDNA is shown as the left black line. The overstretching transition appears to be a transition from dsDNA to ssDNA.**

DNA strands must remain close together during the transition (Wenner *et al.* 2002). The salt dependence data is consistent with both the S-DNA and force-induced melting model. These results are summarized in Figure 13, which shows the effect of changing solution conditions on DNA overstretching. This work has recently been reviewed (Williams *et al.* 2002).

In contrast, dsDNA that is not allowed to rotate freely when stretched does not exhibit an overstretching transition at 65 pN. Instead, a much less cooperative transition at a force of 110 pN is observed (Leger *et al.* 1999). It has been shown that, after unwinding the DNA, the stretching curve exhibits two transitions, one at 50 pN and another at 110 pN and as the amount of DNA unwinding is increased, more of the transition occurs at 50 pN (Leger *et al.* 1999). Overwinding the DNA results in an additional transition at 25 pN, which is attributed to the removal of DNA supercoiling (Leger *et al.* 1999). The currently accepted model is one in which the data are interpreted as transitions between five separate forms of dsDNA (Sarkar *et al.* 2001). However, since it is known that underwound DNA is locally denatured even at low forces (Strick *et al.* 1998), it seems likely that there is DNA denaturation during this transition as well, but this will require further study. In particular, a detailed study of the dependence of these transitions on solution conditions would help to explain the effect of torsional strain on DNA overstretching. Since torsional strain can build up under many physiological conditions (Nelson 1999), this is an important problem to solve. Studies on DNA torsional strain have generally been done using magnetic tweezers, which allow a fixed twist to be applied to DNA molecules by directly controlling the rotation of a magnetic bead in a magnetic trap. However, these studies can also be done using optical tweezers (Smith *et al.* 2002).

Liphardt *et al.* (Liphardt et al. 2001) have recently demonstrated the force-induced unfolding/refolding of small RNA hairpins. In these measurements they unzipped various single-molecule hairpins by pulling on their ends with DNA/RNA hybrid handles attached to beads, as shown in Figure 14. They measured forces of about 15 pN when pulling apart simple double-stranded portions of RNA, similar to measurements of DNA unzipping (Bockelmann et al. 2002). It is interesting to note that the force required to separate the base pairs is different when the DNA or RNA is unzipped (pulling parallel to the base pairs) compared to DNA overstretching experiments in which DNA is pulled perpendicular to the base pairs. The energy measured should be the same in both cases. In fact, the measured energy is very similar. In both cases, the separation of the base pairs before pulling is  $x = 0.34\text{ nm}$ . When the

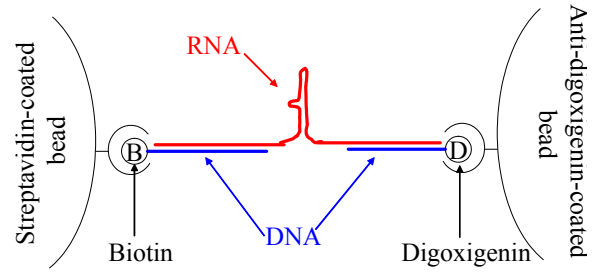


Figure 14. Unzipping a single RNA molecule.

DNA is overstretched, the final separation of the base pairs is  $x = 0.58\text{ nm}$  (see Figure 8). When the DNA or RNA is unzipped, the final separation is  $x = 0.58\text{ nm}$  for each base pair. Thus, for overstretching  $\Delta x_{\text{overstretch}} = 0.24\text{ nm}$  and for unzipping  $\Delta x_{\text{unzip}} = 0.82\text{ nm}$ . If the energy of these processes is the same (i.e. the helix-coil transition free energy), the ratio of the forces should be

$$\frac{F_{\text{unzip}}}{F_{\text{overstretch}}} \approx \frac{\Delta G / \Delta x_{\text{unzip}}}{\Delta G / \Delta x_{\text{overstretch}}} = \frac{\Delta x_{\text{overstretch}}}{\Delta x_{\text{unzip}}} = 0.3, \quad (11)$$

where  $\Delta G$  is the helix-coil transition free energy. We therefore predict from Figure 9 that the force required to unzip DNA should be about 20 pN, in reasonable agreement with the observed unzipping forces.

In these RNA unfolding experiments, the observed pulling and relaxing force curves for some types of hairpin were indistinguishable at low pulling rates, thus indicating thermodynamic reversibility. The area under reversible force/extension curves yields a direct measurement of the equilibrium free energy of structure formation. Such area for a simple 49 bp hairpin structure was in good agreement with the theoretical predictions of the MFOLD method (Zuker 2000). Another structure, the P5abc domain of the tetrahymena ribozyme, forms tertiary contacts in the presence of magnesium. The force-extension curves for this RNA molecule map out its secondary structure and identify metal binding pockets. This will be an extremely valuable technique for the study of RNA folding, as well as RNA-protein interactions.

### 5.3 The interaction of DNA binding proteins with single DNA molecules

Single molecule DNA stretching studies have been used to probe a wide range of DNA-protein interactions. This includes dynamic studies, in which the action of a processive enzyme or molecular motor is directly observed as a function of time (section 5.1), as well as equilibrium studies, from which transition free energies have been derived. In the case of RecA, an accessory protein important for DNA replication and repair, both properties were measured. First, the time dependence of polymerization on a single DNA molecule was directly measured (Hegner *et al.* 1999). Leger *et al.* (Leger et al. 1998) showed that the rate of RecA binding to DNA without ATP hydrolysis increased tremendously at high forces approaching the overstretching transition. Since it is known that in the absence of ATP hydrolysis RecA binds much stronger to ssDNA (McEntee et al. 1981), these experiments support the idea that DNA overstretching induces strand denaturation. After polymerization, the equilibrium elastic properties of RecA/DNA filaments were measured and shown to be dominated by the properties of the RecA protein (Hegner *et al.* 1999).

The experiments described in section 5.2 showed that torsionally constraining DNA significantly alters its elastic behavior. Torsional strain causes the formation of supercoils, in which the double-stranded DNA itself can form complex twisted structures. In the cell, buildup of torsional strain is prevented by the action of an enzyme called topoisomerase. The interaction of topoisomerase with supercoiled DNA has been directly observed using single molecule stretching (Strick et al. 2000). Here the authors were able to watch

the removal of two supercoils during a single enzyme turnover. (In the topoisomerase studies, magnetic tweezers were used rather than optical tweezers.) Finally, a recently study allowed a direct demonstration of the forces exerted by a bacteriophage portal motor when packaging DNA. (Smith *et al.* 2001) The data indicates that an internal force of about 50 pN is built up within the virus capsid when packaging the DNA. These results may shed light on the mechanism by which the virus injects DNA into cells during infection.

The force-induced melting model of DNA overstretching (Rouzina and Bloomfield 2001a) has been used to determine the free energy of the helix-coil transition from DNA overstretching. This is useful for studying DNA-protein interactions, since many proteins operate by binding to DNA and changing its stability. One such protein is HIV-1 nucleocapsid protein (NC), as was recently demonstrated by Williams *et al.* (Williams *et al.* 2001a). NC is a nucleic acid chaperone, which facilitates the rearrangement of the structure of nucleic acids in order to form the lowest energy state (Rein *et al.* 1998). Until now, the mechanism of this activity was not understood. However, Williams *et al.* showed that NC facilitates this rearrangement by significantly lowering the cooperativity and stability of the DNA helix-coil transition. These results show that DNA overstretching is a powerful technique for studying proteins that may lower the helix-coil transition free energy of DNA, including other nucleic acid chaperone proteins, as well as single-stranded binding proteins like *E coli* SSB (Lohman and Ferrari 1994) and T4 Gene 32 (Karpel 1990). In addition, DNA binding drugs that may stabilize or destabilize DNA could be investigated using this method. A study of anti-cancer drugs using AFM showed that these drugs have a significant effect on DNA overstretching (Krautbauer *et al.* 2000). A more recent study showed that the characteristics of the interactions of different types of drugs with DNA could be distinguished by measuring DNA stretching curves. These results suggest that DNA stretching may be used as a tool for drug development (Krautbauer *et al.* 2002).

Given the ability to stretch single RNA hairpin structures, as demonstrated by Liphardt *et al.* (Liphardt *et al.* 2001), single molecule force measurement techniques can be extended to studying the effect of proteins on the helix-coil transition of specific sequences and specific hairpin structures. While both DNA overstretching and nucleic acid unzipping experiments provide a measurement of the free energy of the helix-coil transition (Liphardt *et al.* 2001; Williams *et al.* 2001c), unzipping experiments allow the determination of sequence-specific information as the molecule is unzipped. Thus, the biophysics of sequence-dependent DNA and RNA binding proteins such as transcription factors could be studied in detail using this technique. In addition, single molecule measurements of the kinetics of enzymes that operate on nucleic acids will continue to provide insights into how these molecules function.

Note: Sections of this chapter are taken from (Williams and Rouzina 2002).

## 6. References

- Allemand JF, Bensimon D, Lavery R, Croquette V. 1998. Stretched and overwound DNA forms a Pauling-like structure with exposed bases. *Proc. Natl. Acad. Sci. USA* 95:14152-14157.
- Ashkin A. 1998. Forces of a Single-Beam Gradient Laser Trap on a Dielectric Sphere in the Ray Optics Regime. *Methods in Cell Biology* 55:1-27.
- Baumann CG, Bloomfield VA, Smith SB, Bustamante C, Wang MD, Block SM. 2000. Stretching of Single Collapsed DNA Molecules. *Biophys. J.* 78:1965-1978.
- Baumann CG, Smith SB, Bloomfield VA, Bustamante C. 1997. Ionic Effects on the Elasticity Of Single DNA Molecules. *Proc. Natl. Acad. Sci. USA* 94(12):6185-6190.
- Bockelmann U, Thomen P, Essevez Roulet B, Viasnoff V, Heslot F. 2002. Unzipping DNA with optical tweezers: high sequence sensitivity and force flips. *Biophys J* 82(3):1537-53.
- Clausen-Schaumann H, Rief M, Tolksdorf C, Gaub HE. 2000. Mechanical Stability of Single DNA Molecules. *Biophys. J.* 78:1997-2007.
- Cluzel P, Lebrun A, Heller C, Lavery R, Viovy JL, Chatenay D, Caron F. 1996. DNA: An extensible molecule. *Science* 271:792-794.
- Davenport JR, Wuite GJ, Landick R, Bustamante C. 2000. Single-molecule study of transcriptional pausing and arrest by *E. coli* RNA polymerase. *Science* 287:2497-2500.
- Denk W, Webb WW. 1990. Optical measurements of picometer displacements. *Appl. Opt.* 29:2382-2391.
- Evans E, Ritchie K. 1997. Dynamic Strength of Molecular Adhesion Bonds. *Biophys. J.* 72:1541-1555.

- Gittes F, Schmidt C. 1998. Signals and Noise in Micromechanical Measurements. *Methods in Cell Biology* 55:129-156.
- Hegner M, Smith SB, Bustamante C. 1999. Polymerization and mechanical properties of single RecA–DNA filaments. *Proc. Natl. Acad. Sci. USA* 96:10109-10114.
- Karpel RL. 1990. T4 Bacteriophage Gene 32 Protein. In: Revzin A, editor. *The Biology of Non-Specific DNA-Protein Interactions*. Boca Raton: CRC Press. p 103-130.
- Konrad MW, Bolonick JI. 1996. Molecular dynamics simulation of DNA stretching is consistent with the tension observed for extension and strand separation and predicts a novel ladder structure. *J Am Chem Soc* 118:10989-10994.
- Krautbauer R, Clausen-Schaumann H, Gaub HE. 2000. Cisplatin changes the mechanics of single DNA molecules. *Angewandte Chemie-IE* 39(21):3912-+.
- Krautbauer R, Pope LH, Schrader TE, Allen S, Gaub HE. 2002. Discriminating small molecule DNA binding modes by single molecule force spectroscopy. *FEBS Lett* 510(3):154-8.
- Lebrun A, Lavery R. 1996. Modelling extreme stretching of DNA. *Nucleic Acids Res* 24:2260-2267.
- Leger JF, Robert J, Bourdieu L, Chatenay D, Marko JF. 1998. RecA binding to a single double-stranded DNA molecule: A possible role of DNA conformational fluctuations. *Proceedings of the National Academy of Sciences of the United States of America* 95:12295-12299.
- Leger JF, Romano G, Sarkar A, Robert J, Bourdieu L, Chatenay D, Marko JF. 1999. Structural Transitions of a Twisted and Stretched DNA Molecule. *Phys. Rev. Lett.* 83(5):1066-1069.
- Liphardt J, Onoa B, Smith SB, Tinoco I, Jr., Bustamante C. 2001. Reversible unfolding of single RNA molecules by mechanical force. *Science* 292:733-737.
- Lohman TM, Ferrari ME. 1994. Escherichia coli single-stranded DNA-binding protein: multiple DNA-binding modes and cooperativities. *Ann. Rev. Biochem.* 63:527-70.
- Maier B, Bensimon D, Croquette V. 2000. Replication by a single DNA polymerase of a stretched single-stranded DNA. *Proc. Natl. Acad. Sci. USA* 97(22):12002–12007.
- McEntee K, Weinstock GM, Lehman IR. 1981. Binding of the recA protein of Escherichia coli to single- and double-stranded DNA. *J Biol Chem* 256(16):8835-44.
- Nelson P. 1999. Transport of torsional stress in DNA. *Proceedings of the National Academy of Sciences of the United States of America* 96:14342-14347.
- Olson WK, Zhurkin VB. 2000. Modeling DNA deformations. *Curr. Opin. Struct. Biol.* 10(3):286-97.
- Rein A, Henderson LE, Levin JG. 1998. Nucleic-acid-chaperone activity of retroviral nucleocapsid proteins: significance for viral replication. *Trends Bioch. Sci.* 23:297-301.
- Rief M, Clausen-Schaumann H, Gaub HE. 1999. Sequence-dependent mechanics of single DNA molecules. *Nature Structural Biology* 6(4):346-349.
- Rouzina I, Bloomfield VA. 2001a. Force-induced melting of the DNA double helix. 1. Thermodynamic analysis. *Biophys. J.* 80(2):882-893.
- Rouzina I, Bloomfield VA. 2001b. Force-induced melting of the DNA double helix. 2. Effect of solution conditions. *Biophys. J.* 80(2):894-900.
- Sarkar A, Léger J-F, Chatenay D, Marko JF. 2001. Structural transitions in DNA driven by external force and torque. *Physical Review E* 63:051903.
- Smith DE, Tans SJ, Smith SB, Grimes S, Anderson DL, Bustamante C. 2001. The bacteriophage phi29 portal motor can package DNA against a large internal force. *Nature* 413:748-752.
- Smith SB, Cui Y, Bustamante C. 2002. An Optical-Trap Force Transducer that Operates by Direct Measurement of Light Momentum. *Methods in Enzymology* In press.
- Smith SB, Cui YJ, Bustamante C. 1996. Overstretching B-DNA: The elastic response of individual double-stranded and single-stranded DNA molecules. *Science* 271:795-799.
- Strick TR, Croquette V, Bensimon D. 1998. Homologous pairing in stretched supercoiled DNA. *Proceedings of the National Academy of Sciences of the United States of America* 95:10579-10583.
- Strick TR, Croquette V, Bensimon D. 2000. Single-molecule analysis of DNA uncoiling by a type II topoisomerase. *Nature* 404:901-904.
- Wang MD, Schnitzer MJ, Yin H, Landick R, Gelles J, Block SM. 1998. Force and velocity measured for single molecules of RNA polymerase. *Science* 283:902-907.
- Wenner JR, Williams MC, Rouzina I, Bloomfield VA. 2002. Salt Dependence of the Elasticity and Overstretching Transition of Single DNA Molecules. *Biophys. J.* in press.

- Williams MC, Rouzina I. 2002. Force spectroscopy of single DNA and RNA molecules. *Curr. Opin. Struct. Biol.* in press.
- Williams MC, Rouzina I, Bloomfield VA. 2002. Thermodynamics of DNA Interactions from Single Molecule Stretching Experiments. *Acc. Chem. Res.* 35:159-166.
- Williams MC, Rouzina I, Wenner JR, Gorelick RJ, Musier-Forsyth K, Bloomfield VA. 2001a. Mechanism for nucleic acid chaperone activity of HIV-1 nucleocapsid protein revealed by single molecule stretching. *Proc. Natl. Acad. Sci. USA* 98:6121-6126.
- Williams MC, Wenner JR, Rouzina I, Bloomfield VA. 2001b. The effect of pH on the overstretching transition of dsDNA: Evidence of force-induced DNA melting. *Biophys. J.* 80:874-881.
- Williams MC, Wenner JR, Rouzina I, Bloomfield VA. 2001c. Entropy and Heat Capacity of DNA Melting from Temperature Dependence of Single Molecule Stretching. *Biophys. J.* 80:1932-1939.
- Wuite GJ, Smith SB, Young M, Keller D, Bustamante C. 2000. Single molecule studies of the effect of template tension on T7 DNA polymerase activity. *Nature* 404:103-106.
- Yin H, Wang MD, Svoboda K, Landick R, Block SM, Gelles J. 1995. Transcription against an applied force. *Science* 270:1653-1656.
- Zuker M. 2000. Calculating nucleic acid secondary structure. *Curr. Opin. Struct. Biol.* 10(3):303-10.